Progress in Analysis of Viscous Flow around Podded Propulsor

Zhang Zhi-Rong(1), Hong Fang-Wen(1), Vladimir Kasilnikov(2),Tang Deng-Hai(1)
(1) *China Ship Scientific Research Center,Wuxi,Jiangsu,China,*

(2) *MARINTEK, Trondheim, Norway*

ABSTRACT: A numerical method to predict hydrodynamic characteristics of a pod propulsor has been developed using the general purpose CFD code FLUENT. Sliding mesh technique is used to resolve unsteady interaction between the rotating propeller and stationary housing. A hybrid mesh is adopted in the domain around propeller, while outside the propeller block-structured meshes of hexahedral cells are used. Computations of both the pulling and pushing propulsors have been performed in straight flow. The predicted thrust, torque and housing resistance coefficients are compared with experimental results. A good agreement is observed for the majority of advance coefficients.

1 INTRODUCTION

Pod propulsor is one of the latest innovations in the field of propulsion. Pod propulsor integrates the propulsion system and steering system into one unit, and, since first appearance in early 1990-s, it has been used on many commercial and recreational vessels.

Pod propulsor has many advantages over installation with conventional propeller. It can provide thrust in all directions, giving higher maneuverability to the vessel. The inflow on propeller is more uniform compared to that of conventional propulsion system. This leads to less propeller blade cavitation and lower levels of induced pressure pulses on hull, noise and vibration. Electric-driven pod propulsion systems allow for more flexible machinery arrangement.

The study on hydrodynamic performance of propeller, pod and strut, as well as on flow field around the whole unit is now of increasing importance due to the extensive use of pod propulsors. With pod propulsor taking over conventional rudder/propeller system, it is also important to study on interaction between the propeller and housing, as well as on forces acting on the system at heading angles.

Model tests still remain the most important method to study hydrodynamic performance of pod propulsor. Instrumentation and measuring techniques for pod units have been refined. Various pod models have been tested, regression models and model/full scale extrapolation procedures have been proposed.

In the meantime, numerical methods have been applied, and they are gaining popularity as among researchers as among designers dealing with pod propulsors. The inviscid flow approaches based on vortex-lattice method and panel method, alone or coupled with Euler equation solver, are used for the prediction of pod propeller characteristics in straight flow and at small heading angles, and for the analysis of cavitation on propeller blades. One of the pioneering efforts in applying a potential-based panel method to pod propulsors has been made in (Ghassemi and Allivelli, 1999). Achkinadze et al (2003) have developed a velocity-based quasi-steady panel method improved with semi-empirical viscosity corrections to lift and drag of propeller blade and strut sections, and also to propeller induced velocity field, showing good agreement with test results in terms of propeller thrust and torque, and maneuvering forces acting on the pulling and pushing units, at heading angles up to 15-20 degrees. Krasilnikov et al (2003) have extended this method to predict cavitation domains on podded propeller based on method of equivalent 2D-section. Ma et al (2006) have developed a numerical method to predict the unsteady hydrodynamic forces acting on podded propeller. The solution is based on a vortex-lattice method for the propeller blades and a surface panel method for the pod. Numerical computations are carried out for a 4-bladed propeller mounted on pod, without and with hull. The effect of pod on unsteady propeller forces and moments are discussed based on numerical results. Kinnas et al (2004) have employed a coupled Euler/Vortex-Lattice method to predict the performance of ducted propeller and podded propeller, including the effect of cavitation on propeller and strut. Islam et al (2004) have studied the effects of propeller hub taper angle and pod configuration on propulsive performance by using an existing unsteady panel method code. Inviscid flow methods incur low computation costs and they can easily be used by the designers. At the same time, they imply empirical treatments, as far as viscosity effects are concerned, and require considerable amount of preliminary knowledge/guessing about proper location and geometry of the trailing vortices which affect the results significantly. Predictions of housing resistance and unit forces at large heading angles are, as a rule, poor with these methods.

For pod propulsor the interaction between propeller and housing is very important. Viscosity and unsteadiness play the key roles in this interaction, their contributions increasing for pod propulsor operating in oblique flow where flow separation effects are involved. In viscous CFD, Reynolds-Averaged Navier-Stokes (RANS) methods offer an appropriate compromise between accuracy and computation costs for solving these interaction problems. First RANS applications to pods date back to late 1990-s when Sánchez-Caja et al (1999) analyzed the unsteady flow around a tractor thruster by using the RANS solver FINFLO, in combination with sliding mesh technique. In (Lobachev & Tchitcherine, 2001) scale effects on pod housing resistance were addressed by a RANS solver with propeller represented by an actuator disk with prescribed distribution of body forces to match thrust and torque measured in model tests. Sánchez-Caja et al (2003) investigated into scale effects on pod propulsor using RANS solution for the whole system propeller-pod housing. Calculated flow patterns at full scale are compared to those of model scale. Flow separation on the gondola and strut surfaces is shown to be delayed at full-scale. Forces acting on different components of the tractor unit are shown and compared to model scale results. Hino, Ohashi & Ukon (2003) simulated the flow around ship with pod propulsor using a Navier-Stokes (NS) solver with unstructured mesh. A prescribed body force model is used to represent propeller effects. Krasilnikov et al (2006) presented an iterative coupled RANS(FLUENT)/Panel method where propeller characteristics are not prescribed, but defined in the solution from the panel method analysis of propeller in iteratively elaborated “effective” inflow. Reynolds number effect on propeller characteristics is approximately included. The method is used to predict propeller thrust and torque, housing resistance and propeller/housing interaction coefficients in model and full scale, for the units operating in straight flow. First RANS results for pod propulsors operating in oblique flows were presented in (Junglewitz and El Moctar, 2004). Recently, Koushan & Krasilnikov (2008) presented the results of unsteady RANS simulation of pulling and pushing pod units operating in the range of heading angles between -45 and +45 degrees, using the pre-processing mesh generation code (completely unstructured mesh) developed jointly by CSSRC and MARINTEK and the commercial equation solver of FLUENT. Satisfactory agreement with experimental data in terms of propeller thrust and torque, and total axial and side forces and steering moment on the unit is demonstrated. The aspects of propeller/housing interaction are discussed to explain typical asymmetry in distribution of thrust and torque of pushing propeller versus heading angle. However, large differences between calculated and measured values of the housing resistance are registered.

In this study, the meshing technique described in (Koushan & Krasilnikov, 2008) is refined and applied to the prediction of hydrodynamic characteristics of pulling and pushing pod propulsors in straight flow. Sliding mesh technique is used to solve the unsteady problem of rotating propeller. Propeller thrust and torque, and housing resistance calculated in model scale are validated against test results showing close agreement.

2 NUMERICAL METHOD

2.1 *Governing equations, turbulence model and solver*

The general purpose CFD software FLUENT is used in this study. It solves the RANS equations using a cell-centered finite-volume method. The RANS equations can be written in the following form:

$$\frac{\partial \rho}{\partial t}+\frac{\partial(\rho u_i)}{\partial x_i}=0, \tag{1}$$

$$\frac{\partial(\rho u_i)}{\partial t}+\frac{\partial(\rho u_i u_j)}{\partial x_j}=-\frac{\partial p}{\partial x_i}+\frac{\partial}{\partial x_j}\left[\mu\left(\frac{\partial u_i}{\partial x_j}+\frac{\partial u_j}{\partial x_i}-\frac{2}{3}\delta_{ij}\frac{\partial u_l}{\partial x_l}\right)\right]+\frac{\partial}{\partial x_j}\left(-\rho\overline{u_i' u_j'}\right), \tag{2}$$

where u_i is the i-th Cartesian component of the absolute velocity vector, p is the static pressure, μ is the molecular viscosity, δ_{ij} is the Kronecker delta, and $-\rho\overline{u_i' u_j'}$ is the Reynolds stress. The Reynolds stress must be modeled to close the governing equation by using an appropriate turbulence model.

The SST (Shear Stress Transport) k-ω turbulence model is used for turbulence closure in this paper. The SST k-ω model is one of the most widely used turbulence models for external aero- and hydrodynamics. The SST k-ω model was developed by Menter (1994) to effectively blend the robust and accurate formulation of the k-ω model in the near-wall region with the free-stream independence of the k-ε model in the far field. This model has reportedly better computational performance in flows involving separation, which is an important issue in the analysis of pod propulsor, where separation occurs on the strut and gondola in oblique flows (Koushan and Krasilnikov, 2008). As any isotropic two-equation turbulence model, SST k-ω shows, however, low accuracy in resolving flows near and inside vortical structures. Therefore, one can expect only the integral, overall effect of separation to be captured.

Convection terms in the RANS equations are discretized using a second order upwind scheme, while diffusion terms are discretized using a second order central scheme. Overall solution procedure is based on a SIMPLE-type segregated algorithm. The discretized equations are solved using the Gauss-Seidel iterative procedure, and the algebraic multi-grid method is used to accelerate the solution convergence.

2.2 *Sliding mesh technique*

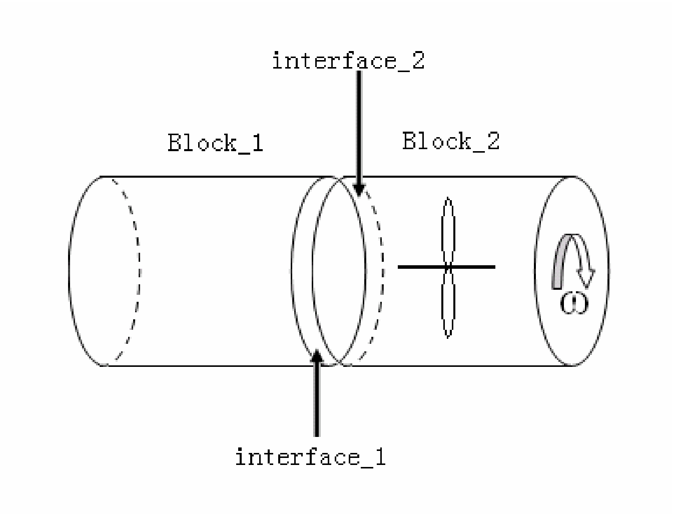

Figure 1. Sliding mesh technique.

Sliding mesh technique is used in this study to simulate the unsteady effect of propeller/pod/strut interaction. The sliding mesh technique is ideally suited for problems involving time-dependent rotor/stator interaction.

In the sliding mesh technique two grids are employed: one for the stationary components and the other for the propeller. The Block_1 in Figure 1 corresponds to stationary body, and the Block_2 corresponds to rotating propeller. The grids of Block_2 move with respect to the stationary grids of Block_1 along the interface surface. The information transfer across the interface surface is done by computing and interpolating fluxes for the faces obtained from the intersection of the neighboring interface zones (interface_1 and interface_2). Mesh blocks do not require alignment on the sliding interface.

2.3 *Modeling of geometry and mesh generation*

The boundary of the computation domain consists of (1) inlet boundary located at 1.0 gondola length ahead of gondola head, (2) exit boundary located at 2.5 gondola lengths from the gondola tail, (3) outer boundary located at 1.5 gondola lengths from the gondola centerline, and (4) the surface of propeller, hub, gondola and strut. The whole domain is divided into the two main sub-domains. One is a cylinder near the propeller blades and the other is outside the propeller, as shown in Figure 2. The outer sub-domain is split into the 30 blocks for mesh generation.

Because of complexity of blade geometry, a hybrid mesh was adopted in the domain around propeller. The mesh was generated using FLUENT pre-processor GAMBIT. Firstly, the blade surfaces were meshed with small triangles, with sides of approximately 0.005D, where D is the propeller diameter. In order to resolve turbulent boundary layer on the wall, four layers of prismatic cells were grown from the blade surface. The wall cell height was approximately 0.001D. Then, the domain is meshed with "size function" which creates condensed mesh around the propeller and gradually increases cell size towards the domains of low velocity gradients. Figure 3 shows the surface mesh on propeller blades and hub surface. This is the first difference from the meshing technique employed in (Koushan & Krasilnikov, 2008) where propeller block consisted only of tetrahedral cells.

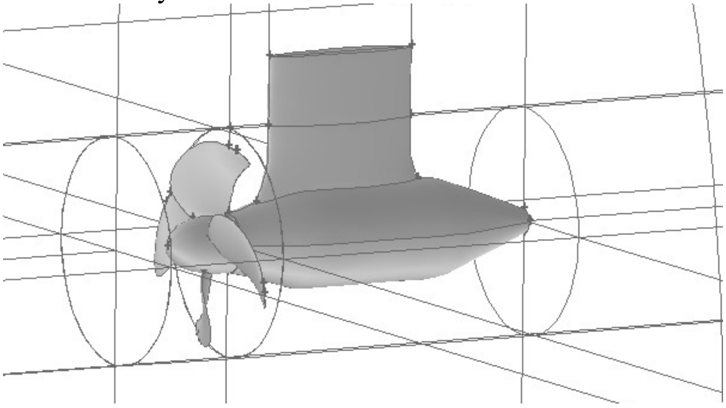

Figure 2. The subdomain near propeller.

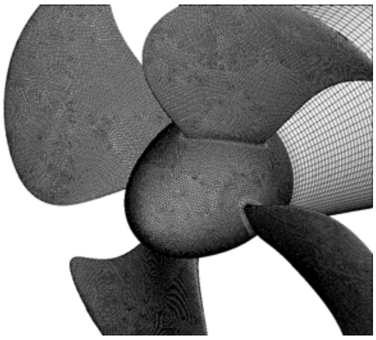

Figure 3. Surface mesh on propeller blades and hub.

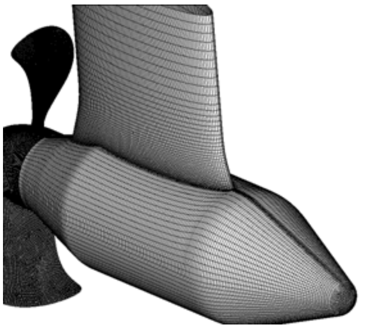

Figure 4. Surface mesh on gondola and strut.

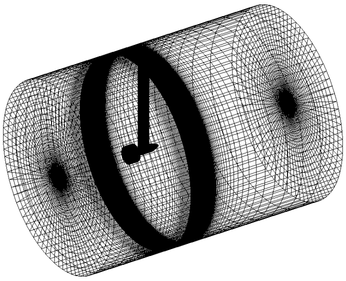

Figure 5. Volume mesh around pod propulsor.

In the domain outside the propeller block, block-structured meshes of hexahedral cells with good orthogonality were used. In order to resolve accurately the boundary layer and predict possible flow separation, fine meshes were used in the near the wall region (enhanced wall treatment). This represents an essential refinement compared to model in (Koushan & Krasilnikov, 2008) where completely unstructured mesh was built and coarse near-wall resolution was used. Figure 4 shows the surface mesh on the gondola and strut. Figure 5 illustrates the volume mesh around the whole proplusor.

2.4 *Initial and boundary condition*

In the present study, the unsteady flow formulation is considered. The uniform inflow velocity field is specified as the initial condition by setting the magnitude of inflow velocity and direction of the inflow at the domain inlet and its outer boundaries, along with turbulence intensity and turbulence viscosity ratio, whereas pressure is extrapolated from the interior nodes. At the domain outlet, static pressure is specified and velocity is extrapolated from the interior nodes. On the blade, hub, gondola and strut surfaces the “no-slip” condition is imposed.

Similar to (Koushan & Krasilnikov, 2008) simulation is performed in two stages. At the first stage, a quasi-steady calculation is carried out using Moving Reference Frame (MRF) method with propeller frozen at vertical top position of the key blade. Converged quasi-steady results are used as initial conditions for time dependent calculation with sliding meshes, at the second stage.

3 RESULTS AND VALIDATION

The present method has been applied to the simulation of the azimuthing pod propulsor tested in the towing tank at MARINTEK, in pulling and pushing modes (Achkinadze et al, 2003), (Koushan & Krasilnikov, 2008). The propulsor is equipped with a four-blade moderate skew propeller. The change from pulling to pushing mode is done by turning the unit to 180 degrees around steering axis, and turning the propeller to keep the direction of propeller rotation, which is right-handed.

The results from quasi-steady and unsteady simulation stages were compared with the measurements. In the tests, propeller thrust and torque were measured by the propeller dynamometer installed on propeller shaft. Experimental housing resistance is defined as a difference between the total axial force measured on the unit and propeller thrust. In the calculations, the axial force acting on the rotating hub is included in propeller thrust, while housing resistance is defined as a sum of the gondola drag and strut drag. Figure 6 shows the comparisons in terms of thrust and torque coefficients of the pulling propeller, and Figure 7 shows the comparison in terms of resistance of the pulling unit. Dimensionless coefficients of thrust, drag and torque are defined as follows:

$$K_{T,X} = \frac{T, F_X}{\rho n^2 D^4}, \quad K_Q = \frac{Q}{\rho n^2 D^5}, \tag{3}$$

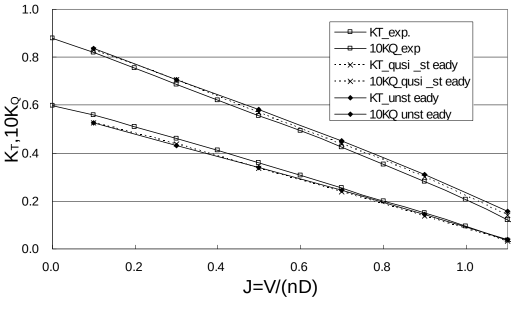

Figure 6. Calculated thrust and torque coefficients for pulling pod propulsor.

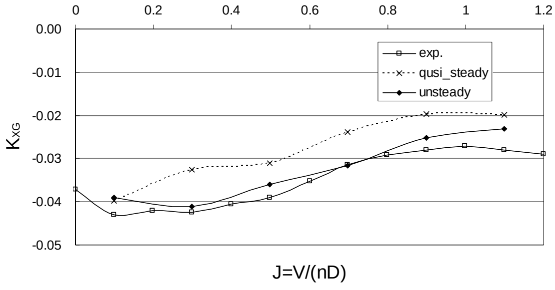

Figure 7. Housing resistance coefficient of pulling pod propulsor.

where T is the thrust, F_X is the drag and Q is the torque; ρ is the density of water; n is the rotational speed of propeller in rps, and D is the diameter of propeller.

Figure 8 shows the relative differences between the quasi-steady predictions and experimental results. Figure 9 shows the relative differences between the unsteady predictions and experimental results. Relative differences for the drag coefficients obtained in quasi-steady and unsteady calculations are shown in Figure 10. It can be seen that propeller K_T is slightly underpredicted, while K_Q is overpredicted in both the quasi-steady and unsteady calculations.

For K_T and K_Q, the differences between quasi-steady and unsteady results are small, especially those for K_T. However, for housing drag, the differences are not negligible. Unsteady results appear to be closer to the measured data since gondola and strut drag are affected by the unsteady phenomena in the flow, such as radial shed vortices in propeller wake and blade-to-blade variation of propeller induced velocity field.

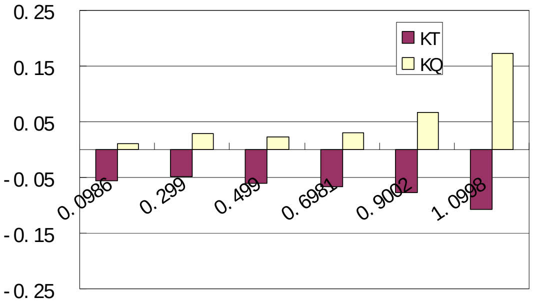

Figure 8. Relative differences between the quasi-steady predictions of thrust and torque and experimental results, for pulling pod propulsor.

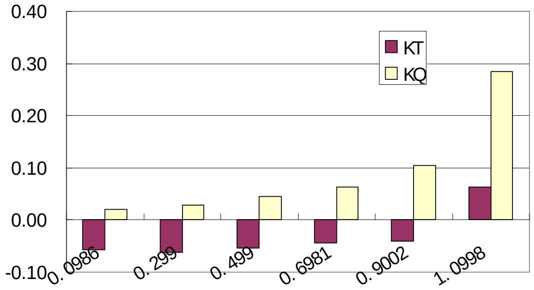

Figure 9. Relative differences between the unsteady predictions of thrust and torque and experimental results, for pulling pod propulsor.

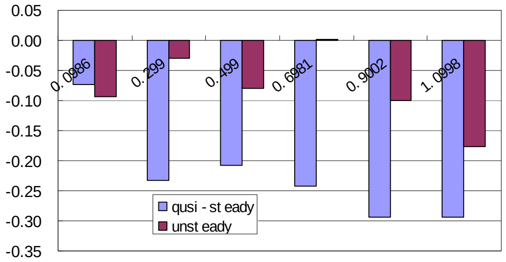

Figure 10. Relative differences in drag coefficient between the quasi-steady and unsteady predictions and experimental results, for pulling pod propulsor.

Figure 11 shows the comparisons in terms of thrust and torque coefficients of pushing propeller. As one can notice, the predicted propeller K_T agrees very well with experimental data in both the quasi-steady and unsteady calculations. The propeller K_Q appears overpredicted.

A likely reason for overprediction in K_Q witnessed for both the pulling and pushing units is seen in the lack of transition model in the RANS solver. More accurately, in the RANS simulation the flow is treated as fully turbulent, while in the model tests laminar flow zones may exist on propeller blades. A calculation based on the assumption of fully turbulent flow regime will probably predict higher values of blade skin friction on the blades, resulting in overpredicted torque and slightly underpredicted thrust, compared to flow with laminar zones. Figures 13 and 14 present the relative differences in the aforementioned cases, for quasi-steady and unsteady calculations, respectively.

As far as drag coefficient of the pushing unit is concerned, the quasi-steady and unsteady predictions are very close, as shown in Figures 12, for absolute values, and in Figure 15, for relative differences. This is explained by the fact that propeller is operating behind the housing, and the unsteadiness of propeller wake does not influence the flow field around gondola and strut significantly.

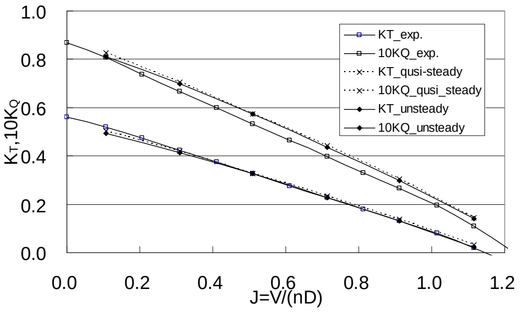

Figure 11. Calculated thrust and torque coefficients for pushing pod propulsor.

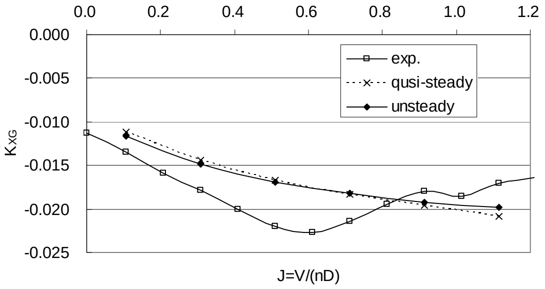

Figure 12. Housing resistance coefficient of pushing pod propulsor.

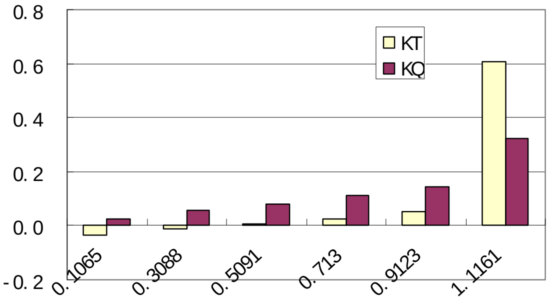

Figure 13. Relative differences between the quasi-steady predictions of thrust and torque and experimental results, for pushing pod propulsor.

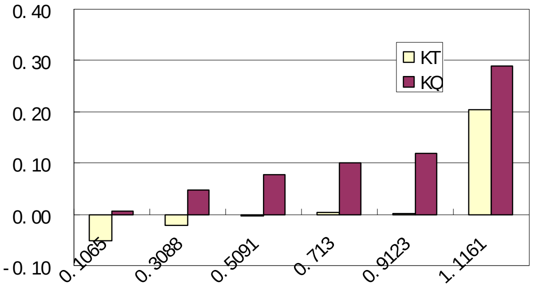

Figure 14. Relative differences between the un-steady predictions of thrust and torque and experimental results, for pushing pod propulsor.

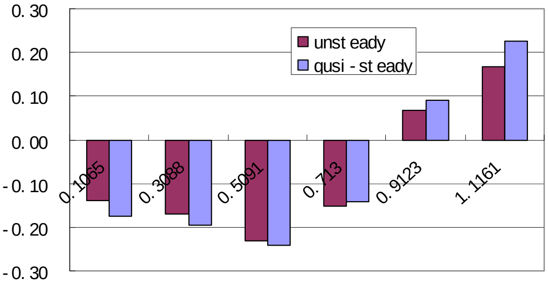

Figure 15. Relative differences in drag coefficient between the quasi-steady and unsteady predictions and experimental results, for pushing pod propulsor.

4 CONCLUDING REMARKS

An unsteady RANS method has been developed to predict hydrodynamics characteristics of pod propulsor using a commercial general purpose CFD code FLUENT. Sliding mesh approach is employed to solve time dependent problem of propeller/housing interaction.

Compared to earlier approach presented in (Koushan & Krasilnikov, 2008), the meshing technique has been refined to resolve more accurately boundary layer flows on propeller blades and pod housing by applying structured mesh blocks in respective domains. Enhanced wall treatment is used instead of coarse near wall resolution.

The characteristics of identical pulling and pushing pod propulsors in straight flow have been predicted, in the range of propeller loading conditions, and compared with experimental data. The comparisons show that predicted propeller thrust agrees very well with the measurements, while propeller torque is overpredicted, for both the pulling and pushing units. The presence of laminar flow zones and laminar-turbulent transition on propeller blades in model tests, which are completely omitted in RANS simulation, may be responsible for the differences observed.

The use of block-structured mesh and fine near-wall resolution allowed for the improvement in prediction of housing resistance, compared to calculation in (Koushan & Krasilnikov, 2008) done on completely unstructured meshes with tetrahedral cells and coarse near-wall resolution.

As far as propeller thrust and torque are concerned, the differences between quasi-steady (MRF, "frozen rotor") and unsteady (sliding mesh) calculations are small. However, unsteady calculation shows much closer agreement with the measurements in terms of housing resistance of the pulling unit, since it takes into account unsteady interaction effects between propeller wake and pod housing.

5. ACKNOWLEDGMENTS

This research was sponsored by the joint industry project "Norwegian Propeller Forum, Phase I".

REFERENCES

Achkinadze, A. S., Berg, A., Krasilnikov, V. I., & Stepanov, I. E. 2003. Numerical Analysis of Podded and Steering Systems Using a Velocity Based Source Boundary Element Method with Modified Trailing Edge, *Propeller/Shafting' 2003 Symposium*, Virginia Beach, VA, USA, September 17-18.

Hino,T., Ohashi,K., & Ukon,Y. 2003. Flow computations around a ship with appendages by an unstructured grid based NS solver, *The 8th International Conference on Numerical Ship Hydrodynamics*, Korea.

Islam,M.,Taylor,R., & Quinton, J. 2004. Numerical Investigation of Propulsive Characteristics of Podded Propellers, *Proceedings of the T-POD2004*, Newcastle, UK.

Junglewitz, A. & El Moctar, O.M. 2004. Numerical Analysis of the Steering Capabilities of a Podded Drive, *Ship Technology Research*, Schiffstechnik, Vol.51.

Kinnas, S. A., Lee, H. S., Gu, H., & Gupta, A. 2004 . Prediction of performance of ducted and podded propellers. *Twenty-Fifth Symposium on Naval Hydrodynamics*, St. John's, Newfoundland and Labrador, Canada.

Koushan, K. & Krasilnikov, V.I. 2008. Experimental and Numerical Investigation of an Open Thruster in Oblique Flow Conditions, *Proceedings of the 27th Symposium on Naval Hydrodynamics*, Seoul, Korea, October 5-10.

Krasilnikov, V.I., Berg, A., & Øye, I.J. 2003. Numerical Prediction of Sheet Cavitation on Rudder And Podded Propellers Using Potential And Viscous Flow Solutions, *Proceedings of the 5th International Symposium on Cavitation CAV2003*, Osaka, Japan, November 1-4.

Krasilnikov, V.I., Ponkratov, D.V., Achkinadze, A.S., Berg, A., & Sun, J. 2006. Possibilities of a Viscous/Potential Coupled Method to Study Scale Effects on Open-Water Characteristics of Podded Propulsors, *Proceeding of the T-POD2006*, IRENav, Brest, France, October 3-5.

Lobachev, M.P. & Tchitcherine, I.A. 2001. The Full-Scale Resistance Estimation for Podded Propulsion System by RANS Method, *Proceedings of the International Symposium on Ship Propulsion*, St Petersburg, Russia, June 19-21.

Ma, Ch., Qian, Z., Yang, C., Zhang, X., Du, D., & Huang, Sh. 2006. Numerical Prediction of Unsteady Performance of Podded Propellers, *Proceedings of the T-POD 2006,* IRENav, Brest, France, October 3-5.

Menter, F.R. 1994. Two-Equation Eddy-Viscosity Turbulence Models for Engineering Applications, *AIAA Journal*, 32(8):1598-1605.

Sánchez-Caja, A., Rautaheimo, P., Salminen, E., & Siikonen, T. 1999. Computation of the Incompressible Viscous Flow around a Tractor Thruster Using a Sliding Mesh Technique, *Proceedings of the 7th International Conference in Numerical Ship Hydrodynamics*, Nantes,France.

Sánchez-Caja, A., Ory, E., Salminen, E., Pylkkanen, J., & Siikonen,T. 2003. Simulation of Incompressible Viscous Flow Around a Tractor Thruster in Model and Full Scale, *Proceedings of the 8th International Conference on Numerical Hydrodynamics*, Busan, Korea.